

1 **A Post-2013 Drop-off in Total Ozone at a Third of Global Ozone-sonde Stations: ECC Instrument**
2 **Artifacts?**

3 **Ryan M. Stauffer^{1,2}, Anne M. Thompson², Debra E. Kollonige^{3,2}, Jacquelyn C. Witte^{2*}**
4 **David W. Tarasick⁴, Jonathan Davies⁴, Holger Vömel⁵, Gary A. Morris⁶, Roeland Van**
5 **Malderen⁷, Bryan J. Johnson⁸, Richard R. Querel⁹, Henry B. Selkirk^{10,2}, Rene Stübi¹¹, and**
6 **Herman G. J. Smit¹²**

7 ¹Earth System Science Interdisciplinary Center, University of Maryland, College Park, MD,
8 USA

9 ²Atmospheric Chemistry and Dynamics Lab, NASA/GSFC, Greenbelt, MD, USA

10 ^{*}Now at National Center for Atmospheric Research Earth Observations Laboratory, Boulder,
11 CO, USA

12 ³Science Systems and Applications, Inc., Lanham, MD, USA

13 ⁴Environment and Climate Change Canada, Downsview, ON, CA

14 ⁵National Center for Atmospheric Research Earth Observations Laboratory, Boulder, CO, USA

15 ⁶St. Edwards University, Austin, TX, USA

16 ⁷Royal Meteorological Institute of Belgium, Uccle (Brussels), Belgium

17 ⁸Global Monitoring Division, NOAA Earth System Research Laboratory, Boulder, CO, USA

18 ⁹National Institute of Water & Atmospheric Research (NIWA), Lauder, NZ

19 ¹⁰Universities Space Research Association, Columbia, MD, USA

20 ¹¹Federal Office of Meteorology and Climatology, MeteoSwiss, Aerological
21 Station, Payerne, Switzerland

22 ¹²Institute of Chemistry and Dynamics of the Geosphere: Troposphere, Jülich Research Centre,
23 Jülich, Germany

24

25 Corresponding author: Ryan M. Stauffer (ryan.m.stauffer@nasa.gov)

26 **Key Points:**

- 27 • We report a drop in ozonesonde total column O₃ of 3-7 % relative to independent
28 measurements at a third of sites beginning around 2014
- 29 • Comparisons with satellite stratospheric O₃ profiles show the artifact loss peaking at 5-
30 10 % or more in the middle and upper stratosphere

- 31 • Changes in the ozonesonde instrument are apparently associated with the drop-off, but no
32 single factor appears to be the cause

33 Keywords: ECC Ozonesonde, Aura, OMI, MLS, Suomi-NPP, OMPS

34 Index Terms: 0394, 0365, 9815

35 **Abstract**

36 An international effort to improve ozonesonde data quality and to reevaluate historical
37 records has made significant improvements in the accuracy of global network data. However,
38 between 2014 and 2016, ozonesonde total column ozone (TCO; O₃) at 14 of 37 regularly
39 reporting stations exhibited a sudden drop-off relative to satellite measurements. The ozonesonde
40 TCO drop is 3-7 % compared to satellite and ground-based TCO, and 5-10 % or more compared
41 to satellite stratospheric O₃ profiles, compromising the use of recent data for trends, although
42 they remain reliable for other uses. Hardware changes in the ozonesonde instrument are likely a
43 major factor in the O₃ drop-off, but no single property of the ozonesonde explains the findings.
44 The bias remains in recent data. Research to understand the drop-off is in progress; this letter is
45 intended as a caution to users of the data. Our findings underscore the importance of regular
46 ozonesonde data evaluation.

47 **Plain Language Summary**

48 Balloon-borne ozonesondes provide accurate measurements of atmospheric ozone (O₃)
49 from the surface to above 30 km with high vertical resolution. Dozens of global stations have
50 regularly launched ozonesondes for decades, and they provide vital information for improving
51 O₃-measuring satellite algorithms, tracking recovery of the stratospheric O₃ layer, and our
52 understanding of surface to lower stratospheric O₃ changes in an evolving climate. We present
53 the discovery of an apparent instrument artifact that has caused total column O₃ measurements

54 from about a third of global stations to drop by 3-7 % starting in 2014-2016, limiting their
55 suitability for calculating O₃ trends. Work is underway to solve the problem, but the exact cause
56 of the drop is still unknown. This letter serves as a caution to the community of ozonesonde data
57 users.

58

59 **1 Background: The Ozonesonde Instrument and Data Quality Assurance**

60

61 The electrochemical concentration cell (ECC) ozonesonde measures ozone (O_3) profiles
62 from the surface through the mid-stratosphere (~ 5 hPa). Ozone is measured via a chemical
63 reaction from bubbling ambient O_3 into a two-chamber electrochemical cell containing a
64 potassium iodide (KI) solution (sensing solution type or SST, which refers to the solution KI and
65 pH buffer concentration; see Table 1). The ECC is launched on a weather balloon coupled to a
66 radiosonde that transmits O_3 partial pressure simultaneously with pressure, temperature,
67 humidity (PTU), and GPS-derived wind data to a ground station approximately once a second.
68 With a 20-30 s response time, the effective vertical resolution of the O_3 signal is ~ 150 m.

69 Because each ozonesonde is a new instrument that must be prepared before launch, it is
70 essential to standardize instrument preparation, operations, and the treatment of raw data. In the
71 past decade, a panel of researchers have engaged in both individual and collective tests of
72 instrumentation, meeting regularly to discuss quality assurance and to develop standard operating
73 procedures (SOP) in an activity designated Assessment of SOP for Ozonesondes (ASOPOS).
74 Current SOP were published in **Smit and ASOPOS (2014)**. The main sources of instrument
75 variability are the instrument type (there are two major manufacturers of ECC instruments,
76 which we call “Type1” and “Type2”), the composition of the SST, conditioning protocol, and
77 post-processing; these parameters are given in the metadata for each record.

78 ASOPOS has also published guidelines for reprocessing sonde data records that may be
79 affected by deliberate or inadvertent ECC preparation changes. For example, the ASOPOS
80 recommendation is to deploy each ECC type with a different SST, even though the two types
81 operate on the exact same measurement principle. If a station changes only one of these

82 variables, the resulting step change in O₃ is considered an instrumental artifact. Reprocessing is
83 carried out to compensate for such changes, and the data are said to be homogenized (**Smit and**
84 **ASOPOS, 2012; Deshler et al., 2017**). Both the SOP and reprocessing guidelines are based on
85 laboratory (**Smit et al., 2007**) and field tests (**Deshler et al., 2008**) in which different sensors are
86 compared with a standard O₃ reference photometer. In the lab, tests are made with 2-4 ECC
87 sensors operating in a closed chamber that simulates a standard profile over a 2-hr “flight.” Field
88 tests compare instruments on a single gondola launched with a balloon capable of lifting the
89 payload to ~30 km.

90 During the period 2013 through 2017 data from more than 25 ozonesonde stations were
91 reprocessed (**Tarasick et al., 2016; Van Malderen et al., 2016; Thompson et al., 2017; Witte**
92 **et al., 2017; Sterling et al., 2018; Witte et al., 2019**). In general, the reprocessed data show
93 significant improvements in comparisons with independent total column ozone (TCO)
94 measurements. Reprocessed data at 12 of 14 SHADOZ stations agree to within 2 % of satellite
95 and ground-based TCO measurements (**Thompson et al., 2017**), compared to offsets > 8 % at
96 half of the stations through 2004 in **Thompson et al. (2007)**. Improvements in tropical mid-
97 stratospheric O₃ values also led to better agreement with Microwave Limb Sounder (MLS)
98 profiles (2005-2017; **Witte et al., 2017**).

99 In spite of the reprocessing successes, the homogenized data for two tropical stations
100 (Costa Rica and Hilo) displayed sharp 5 % drop-offs in TCO relative to satellite measurements
101 after 2014; at Hilo a simultaneous discrepancy appeared relative to the Mauna Loa Dobson
102 spectrometer (**Thompson et al., 2017; Sterling et al., 2018**). The drop-off was also observed in
103 the original datasets, ruling out the reprocessing as the cause. In contrast, NOAA’s Boulder, CO,
104 site, which used the same instrumentation and SST, did not appear to be similarly affected.

105 Hypothesized causes for these findings, e.g., hardware changes in the 2011-2016 period (the
106 company manufacturing Type1 ECCs changed ownership twice) or NOAA's non-standard SST
107 used at the above-mentioned sites, were tested along with other variables in a new series of
108 chamber tests (JOSIE; Jülich Ozonesonde Intercomparison Experiments) in late 2017. Initial
109 results from the 80 chamber profiles in JOSIE-SHADOZ could not explain the drop-off behavior
110 (**Thompson et al., 2019**), and the cause remained unsolved.

111 Because ozonesonde profiles are relied upon as the foundation for satellite O₃ retrievals
112 and validation, we re-examine the agreement among sonde, satellite, and ground-based TCO
113 with two more years of data from the SHADOZ and NOAA networks to determine if the drop-
114 offs reported in **Thompson et al. (2017)** and **Sterling et al. (2018)** persist. We also extend these
115 analyses to the global network during the Aura satellite era of October 2004 to present. We find
116 that over a third of these 37 stations exhibit an instrumental artifact drop-off in TCO after 2013,
117 caused by a decline in ECC stratospheric O₃ measurements. Instrumental factors are investigated
118 but no definitive explanation for these findings has yet emerged. In **Section 2** data sources and
119 statistical methods are described. **Section 3** describes results and potential changes to the ECC
120 instrument and factors that require further investigation. **Section 4** is a summary and
121 recommendations for use of data affected by the ECC O₃ drop-off.

122

123 **2 Data and Methods**

124

125 **2.1 ECC Ozonesonde Data**

126

127 We selected a total of 37 global ECC ozonesonde sites based on the availability of
128 consistent and up-to-date records during the Aura period from October 2004 to present (i.e. data
129 available within the last few years; an exception is Watukosek which ended in October 2013) to
130 analyze the recent drop in ECC TCO measurements. Currently, 28 of the sites launch Type1
131 ECCs, and nine launch Type2. Some sites have previously changed ECC types, SST, or both, so
132 the most recent metadata are listed in **Table 1**. The primary evaluation of ozonesonde data is
133 with TCO and stratospheric O₃ measurements from NASA's Aura satellite; sample numbers
134 listed in **Table 1** are from the Aura period only. The ozonesonde data are not normalized to a
135 TCO measurement or an outside data source. We calculate ECC TCO amounts by integrating the
136 ozonesonde O₃ up to 10 hPa or balloon burst, whichever is greater in pressure, and add the
137 **McPeters and Labow (2012)** climatological residual O₃ to that amount. We do not calculate the
138 TCO amount for ozonesondes that fail to reach 30 hPa.

139

140 **2.2 Satellite and Ground-Based Data**

141

142 Satellite TCO measurements are from the Aura Ozone Monitoring Instrument (OMI v8.5;
143 **McPeters et al., 2008; MCPeters et al., 2015**) and the Suomi-NPP Ozone Mapping Profiler
144 Suite (OMPS v2; **McPeters et al., 2019**). To identify “coincident” satellite overpasses, we limit
145 Level 2 TCO data to within 8 hours and 100 km of the ozonesonde measurement. Sensitivity
146 tests on our screening of coincident satellite TCO data by limiting comparisons based on cloud
147 fraction or a smaller overpass distance to the ECC site had negligible effects on the statistics
148 (less than 1 % change in overall OMI/ECC TCO agreement). Stratospheric O₃ profile
149 measurements are from Aura MLS (**Froidevaux et al., 2008**). We use MLS v4.2 Level 2 O₃ data

150 averaged within one day and 5° latitude and 8° longitude of the ozonesonde launch. MLS data
151 are screened according to the v4.2 Level 2 MLS Data Quality document (**Livesey et al., 2018**).

152 The OMI and OMPS TCO measurements compare well with the series of Solar
153 Backscatter Ultraviolet instruments and are suitable for TCO trend analysis (**McPeters et al.,
154 2015; 2019**). Aura MLS O₃ measurements in the stratosphere exhibit little drift – the v3.3
155 measurements are stable to within 1.5 % per decade (**Hubert et al. 2016**; it is presumed the v4.2
156 data used here have similar stability). Thus, these three satellite instruments are suitable to detect
157 significant changes in the ECC ozonesonde network. Our primary ECC comparisons are with
158 OMI and MLS because of their > 15 year record. OMPS reinforces the OMI and MLS results.

159 Twenty-three of the 37 ECC sites have a co-located ground-based TCO instrument
160 (**Table 1**). Most sites have a Brewer or Dobson spectrophotometer (or both at Hilo and Tateno);
161 Réunion uses a SAOZ UV-visible spectrometer. ECC TCO comparisons with all three ground-
162 based instrument types are found in **Thompson et al. (2017)**.

163

164 **2.3 Defining the ECC O₃ Drop-off: Example Sites**

165

166 To characterize the O₃ drop-off, we separate the sites with unambiguous drops in TCO,
167 which we call “affected” sites, from those called “reference” sites. Affected sites are defined as
168 follows: At each site, the average difference between ECC and OMI TCO for 2004-2013 (nearly
169 a decade of measurements) is computed. A moving, 100-sample average of differences between
170 ECC and OMI TCO for the entire record is compared to the 2004-2013 value. If the moving
171 average falls more than 3 % below the 2004-2013 value, the site is identified as having a drop-
172 off at that date. The identified drop-off dates may occur a few months after a visual “breakpoint”

173 in the time series of ECC and OMI comparisons, but the 100-sample moving average ensures
174 that any drop-off in ECC TCO is sustained over many ozonesonde profiles and is not a
175 temporary feature. The date of drop-off and maximum TCO drop relative to OMI are listed for
176 affected sites in Table 1. For example, **Figure 1a** displays a sudden drop-off relative to OMI at
177 Kelowna in November 2014. The ECC TCO averaged 4 % higher than OMI from 2004-2013.
178 The 100-sample moving average fell to +1 % in November 2014, and fell as low as -0.7 % in
179 December 2016 for a maximum 4.7 % drop (Table 1).

180 The drop-off is identified at Hilo in March 2015 and at Costa Rica in December 2015
181 (**Figure 1b, c**). Hilo and Costa Rica exhibit maximum drop-offs of 4.0 and 6.2 % relative to
182 OMI. The percent differences between ozonesonde and MLS stratospheric O₃ in the top panels
183 of **Figure 1** show that the drop in ECC O₃ relative to MLS is coincident with the TCO drop.

184

185 **3 Results and Discussion**

186

187 **3.1 Sites Affected by the ECC O₃ Drop-off**

188

189 Using the criterion of a > 3 % TCO drop relative to OMI, we find that 14 of 37 sites are
190 affected by a TCO drop-off. **Table 1** lists the affected sites in bold including the maximum TCO
191 drop relative to OMI computed using the 100-sample moving average. A map of all sites
192 examined, with affected sites colored according to the magnitude of TCO drop-off, is shown on
193 **Figure 2**. We define the drop in TCO as relative to OMI because some sites previously exhibited
194 a high bias compared to satellites, with the drop-off actually leading to closer agreement with
195 OMI (e.g. Kelowna in **Figure 1a**).

196 Dates of the drop in TCO measurements range from January 2014 at San Cristóbal to
197 January 2017 at Edmonton. All but one (Natal) of the affected sites use Type1 ECCs. The
198 magnitude of the TCO drop-off varies considerably. The drop in TCO at Nairobi is a relatively
199 modest 3.2 %, whereas a change of 7.4 % is observed at Yarmouth. It appears that there are two
200 clusters of affected sites, in the tropics and in Canada, with most mid-latitude sites remaining
201 unaffected by a drop-off. In summary, there is inconsistency in TCO drop-off amount, and the
202 drop-off is not a universal problem.

203 Comparisons similar to **Figure 1** for the remaining 34 sites in **Table 1** are found in the
204 Supplementary Material in **Figures S1a-k and S2a-w**. We note that individual sites show
205 periods of high or low bias compared to OMI and MLS (e.g. Madrid's high bias for a portion of
206 2009; **Figure S2h**). However, our focus is on sudden drops in O₃ that persist for more than 2 or 3
207 years in the most recent record, because this appears to be a widespread pattern, affecting much
208 of the global network.

209

210

211 **3.2 Comparisons with Aura MLS Stratospheric O₃**

212

213 Closer comparison of ECC and MLS O₃ profiles in the stratosphere is warranted given
214 the coincidence between the ECC drop-off relative to OMI and OMPS TCO, and apparent ECC
215 drop-off relative to MLS O₃ in **Figure 1**. **Figure 3a** shows a composite of comparisons between
216 MLS and ECC ozonesonde stratospheric O₃ at the 14 affected sites before and after the identified
217 drop-off (dates in **Table 1**). Prior to the drop-off at the 14 affected ECC sites, stratospheric O₃
218 biases compared to MLS follow the zero line in **Figure 3a** (blue colors). After the drop-off in

219 TCO, the ECC measurements shift 5-10 % lower relative to MLS (red colors), occasionally
220 reaching > 20 % low above 10 hPa (the 25th percentile value at the 6.81 hPa MLS level is -20.3
221 %). **Figure 3b** and **3c** show similar statistics for the reference Type1 and Type2 sites. The
222 comparisons with MLS profiles are split into 2004-2013 and 2014-2019, near the time when
223 many affected sites exhibit the drop-off. **Figure 3b** and **3c** show that there is no comparable
224 drop-off in stratospheric O₃ at the Type1 and Type2 reference sites. **Figure 3a** indicates that the
225 stratospheric O₃ drop-off is the major contributor to the TCO offsets with OMI and OMPS. Time
226 series of ECC comparisons with OMI TCO and MLS partial stratospheric column O₃ in **Figure**
227 **S3** demonstrate that the drop-off in ECC stratospheric O₃ exactly coincides with the TCO drop.
228 At this point, a similar drop-off in tropospheric O₃ has not been detected and is presumed to be
229 insignificant. Exceptions are two stations, Costa Rica and Hilo, which may be reading low in
230 recent years in the troposphere due to occasional volcanic SO₂ interference (e.g. **Morris et al.,**
231 **2010**). That is beyond the scope of our study.

232

233 **3.3 Potential ECC Instrument Factors in the O₃ Drop-off**

234

235 The ECC O₃ drop-off has been quantified against satellite TCO and satellite O₃ profiles
236 (**Thompson et al., 2017; Sterling et al., 2018**; ground-based comparisons to follow in Section
237 3.5). Thus, we rule out geophysical factors as the only cause; the drop-off seems to be an
238 instrument artifact, so we consider potential instrumental contributions. Each ECC is built from a
239 number of components that may change over time as the manufacturer or manufacturers'
240 suppliers change. For example, the Type1 instrument changed manufacturer twice between 2011
241 and 2016. Components that could change and affect the ECC measurements include the

242 chambers holding the sensing solution, the ion bridge between the two cells, the air intake pump,
243 the constant-speed motor, batteries, and the platinum electrodes. A 3-7 % change of response
244 could be caused by loss of O₃ or of molecular iodine to the ECC chamber walls, losses through
245 the internal resistance of the cell, or in-flight changes in the pump and motor efficiency with
246 pressure. The sensing solution composition and the radiosonde model (and interface) are
247 additional considerations (Section 3.6). The ECC serial number is used to evaluate potential
248 instrument/component changes over time.

249 **Figure 4** shows ECC TCO offsets with OMI and OMPS separated by the 13 affected (red
250 on **Figure 4**) and 15 reference (blue on **Figure 4**) Type1 sites. Median, 25th and 75th percentile
251 statistics are shown for every 1000 serial numbers (e.g. 24K = 24000-24999). The affected sites
252 show a low bias for 25K or higher serial numbers, abruptly dropping from a median TCO bias
253 compared to OMI and OMPS of +1.6 % (24K), to -2.6 % (25K). The inconsistency in timing of
254 the ECC drop-off at affected sites is partly due to when the site begins launching serial numbers
255 25K and above. The reference sites show no such drop, and, in fact, no recent serial number set
256 since 24K has a median bias larger than -1.5 % (30K) for the 12 reference sites. The affected
257 sites show significant negative biases for all serial numbers from 25K to 35K, with a maximum
258 median low bias of -5.4 % for 31K serial numbers. **Figure 4** shows the history of good
259 ECC/satellite agreement at affected Type1 sites throughout the Aura record since October 2004
260 and prior to the 25K serial numbers, although there are indications of some low-biased
261 measurements from serial numbers 20-22K. The largest deviation for reference Type1 sites is the
262 +1.7 % median bias for 16K serial numbers (**Figure 4**). In summary, before the TCO drop-off at
263 the affected sites, the ECC TCO comparisons with satellite measurements averaged within 1 or 2
264 %, and comparisons at reference sites remain, on average, within 1 or 2 %.

265 **Figure 4** shows that reference and affected Type1 sites were both launching ECCs with
266 similar serial numbers, so it is puzzling why they show such large discrepancies in their
267 comparisons with satellite TCO after serial number 24K. This commingling of good and poorly-
268 performing Type1 serial numbers, which appear to be distinguishable only by site, tells us that
269 the ECC O₃ drop-off is not due to manufacturing issues for the Type1 ECC alone and that at least
270 one additional secondary factor must play a role in its occurrence.

271

272 **3.4 Stations with Type2 ECCs**

273

274 We examined nine Type2 ECC ozonesonde sites for a drop-off and sudden low TCO
275 bias. Statistics of the TCO offset between reference Type2 ECCs and OMI and OMPS are also
276 shown on **Figure 4** in grey. Note that the similar serial numbers between Type1 and Type2
277 ECCs are a coincidence. The Type2 comparisons show no abrupt downward shift in agreement
278 with satellite TCO as seen at the affected Type1 sites in **Figure 4**. An exception is at Natal
279 (**Figure S1h**).

280

281 **3.5 ECC Comparisons with Ground-Based TCO Measurements**

282

283 Of the 37 sites analyzed here, 23 have ground-based TCO measurements to compare
284 against the ECCs (**Table 1**). Example time series of the comparisons between ECCs and the
285 Brewer at Churchill, and the Brewer and Dobson at Hilo are shown in **Figure S4**. The ground-
286 based TCO measurements near Hilo are taken at Mauna Loa (3405 m), which explains why the
287 ECC TCO is higher than the Brewer and Dobson prior to the March 2015 drop-off. Statistics

288 similar to **Figure 4** for the ground-based TCO comparisons are shown in **Figure S5**. The ECC
289 TCO drop-off relative to the ground-based instruments at affected Type1 sites is ~3-4 % after
290 20-25K serial numbers in **Figure S5**. The ground-based comparisons with reference Type1 and
291 Type2 sites are quite variable, and the difference in behavior of affected Type1 ECCs is not as
292 apparent in the ground-based comparisons as it is in the satellite TCO comparisons. This is
293 because several affected sites like Costa Rica, Ascension, Kelowna, and Yarmouth do not have
294 ground-based TCO instruments. Spectrometer data at some affected Canadian sites are also
295 limited by low winter sunlight.

296

297 **3.6 Possible Sources of the Drop-Off**

298

299 Around 2010-2012, most of the affected ozonesonde sites examined here switched from
300 the Vaisala RS-80 to RS-92 radiosonde, or from RS-80 to the InterMet iMet radiosonde. The
301 radiosonde pressure measurements affect the ECC O₃ calculation and altitude registration, so a
302 change from non-GPS RS-80 to GPS-enabled RS-92 and iMet radiosondes can lead to pressure
303 measurement changes, which translate to O₃ changes (**Steinbrecht et al., 2008; Stauffer et al.,**
304 **2014; Inai et al., 2015**). Some sites (e.g. Lauder in 2015) switched radiosondes again from RS-
305 92 to the RS-41. An example of an RS-80 to iMet transition at Hilo is shown in **Figure S6**. There
306 is a shift in mid-stratospheric pressure and temperature measurements with the transition to iMet
307 in 2011-2012, but this change occurs more than two years before the Hilo low O₃ bias in March
308 2015. Similar mismatches between radiosonde changes and the ECC drop-off are found at other
309 sites. Costa Rica switched from RS-80 to iMet radiosondes in 2012-2013, but the drop-off did
310 not occur until December 2015 (**Thompson et al., 2017**). Nairobi switched from RS-80 to RS-92

311 radiosondes in 2010, but there was no drop-off until July 2016. We therefore rule out radiosonde
312 changes as the primary cause of the ECC O₃ drop-off.

313 The drop-off is found at sites that use a variety of SSTs (**Table 1**) and three different
314 radiosonde types (RS-92 or 41 and iMet). Sites that are seemingly unaffected, e.g. Trinidad
315 Head, Boulder, and Huntsville, all use the same 1.0 % KI with 1/10th buffer SST and iMet
316 radiosonde combination as Hilo and Costa Rica (**Figure 1**). We have not fully explored the
317 effects of different SSTs on the O₃ drop-off, but given that all three SSTs currently in use are
318 affected (**Table 1**), it does not appear that SST is the main factor.

319 The ASOPOS 2.0 panel is performing additional experiments and analyses to identify
320 possible sources of the O₃ drop-off. Tests include examining the different radiosonde interface
321 boards and batteries used on Type1 ECC sondes, reviewing site ECC preparation procedures,
322 and experiments with older Type1 ECCs manufactured before the drop-off began. Possible
323 changes in behavior of the pump, pump motor, or batteries at low stratospheric pressures and
324 temperatures, are obvious candidate factors and have been considered, but preliminary results
325 have not identified significant differences. Both Type1 and Type2 ozonesondes, four different
326 sensing SSTs, and varying preparation procedures were tested in the 2017 JOSIE-SHADOZ
327 experiment (**Thompson et al., 2019**), and a preliminary analysis did not reveal any signs of the
328 drop-off in those data. In-depth analysis of the 80 profiles from JOSIE-SHADOZ should help
329 identify the causes and magnitudes of contributing factors like SST to the ECC O₃ drop-off.

330

331 **4 Summary and Recommendations for Affected Data**

332

333 Since 2014-2016, we have observed a drop-off in ECC ozonesonde TCO and
334 stratospheric O₃ at 14 ECC global ozonesonde sites, 13 of which launch Type1 ECC
335 ozonesondes. The TCO drop is 3-7 % compared to OMI TCO measurements, and the
336 stratospheric O₃ drop can be greater than 10 % compared to MLS O₃ profiles in the mid-
337 stratosphere. The low bias is notably absent at half of the 28 Type1 sites that we examined.
338 Except for Natal, there is no significant drop-off or change in bias for Type2 ECC ozonesondes
339 during similar years. Because the drop-off varies greatly from site-to-site, it is likely that it is
340 influenced by station-specific procedures yet to be identified. The ECC O₃ drop-off has more
341 than one single cause (i.e. both instrument- and station-specific influences).

342 Affected data archives such as SHADOZ (<https://tropo.gsfc.nasa.gov/shadoz/>), the World
343 Ozone and Ultraviolet Data Centre (WOUDC.org), and the Network for the Detection of
344 Atmospheric Composition Change (NDACC; ndaccdemo.org) are posting caveats and flagging
345 affected profiles. Ongoing research is directed at identifying the cause of the low O₃ bias.

346 We emphasize that all reprocessed data are expected to be more accurate than
347 unhomogenized data. For affected sites, data before the drop-off are highly reliable and even
348 affected data are accurate for satellite validation and algorithms, process studies, and model
349 evaluation because the apparent drop-off averages less than 5 %. However, the affected data are
350 judged not appropriate for calculations of TCO or stratospheric trends or satellite drift.

351

352 **Acknowledgments**

353 Funding for this work was provided through support of SHADOZ by the NASA Upper Air
354 Research Program (UARP; Dr. Kenneth Jucks program manager) to NASA/GSFC (A. M.
355 Thompson, PI). SHADOZ v6.0 ozonesonde data were downloaded from the NASA/GSFC
356 archive at <https://tropo.gsfc.nasa.gov/shadoz/>. Canadian reprocessed ozonesonde data were
357 provided by co-author D. Tarasick, and reprocessed Uccle ozonesonde data were provided by co-
358 author R. Van Malderen. NOAA ozonesonde data (Boulder, Huntsville, and Trinidad Head) were
359 downloaded at <ftp://aftp.cmdl.noaa.gov/data/ozwv/Ozonesonde/>. All other ozonesonde data and
360 all ground-based TCO data are available at the World Ozone and Ultraviolet Data Centre
361 (WOUDC; <https://woudc.org/data/explore.php?lang=en>). Aura MLS v4.2 Level 2 O₃ overpass
362 data were downloaded at
363 <https://avdc.gsfc.nasa.gov/pub/data/satellite/Aura/MLS/V04/L2GPOVP/O3/>. OMI and OMPS
364 Level 2 TCO overpass data were downloaded at
365 <https://avdc.gsfc.nasa.gov/pub/data/satellite/Aura/OMI/V03/L2OVP/OMTO3/> and
366 https://avdc.gsfc.nasa.gov/pub/data/satellite/Suomi_NPP/L2OVP/NMTO3-L2/.

367

368 **References**

- 369 Deshler, T., et al. (2008), Atmospheric comparison of electrochemical cell ozonesondes from
370 different manufacturers, and with different cathode solution strengths: The Balloon
371 Experiment on Standards for Ozonesondes, *J. Geophys. Res.*, 113, D04307,
372 doi:10.1029/2007JD008975.
- 373 Deshler, T., R. Stuebi, F. J. Schmidlin, J. L. Mercer, H. G. J. Smit, B. J. Johnson, R. Kivi, R., and
374 B. Nardi (2017), Methods to homogenize electrochemical concentration cell (ECC)
375 ozonesonde measurements across changes in sensing solution concentration or ozonesonde
376 manufacturer, *Atmos. Meas. Tech.*, 10, 2021–2043, doi:10.5194/amt-10-2021-2017.
- 377 Froidevaux, L., et al. (2008), Validation of Aura Microwave Limb Sounder stratospheric ozone
378 measurements, *J. Geophys. Res.*, 113, D15S20, doi:10.1029/2007JD008771.
- 379 Hubert, D., et al. (2016), Ground-based assessment of the bias and long-term stability of 14 limb
380 and occultation ozone profile data records, *Atmos. Meas. Tech.*, 9, 2497–2534,
381 <https://doi.org/10.5194/amt-9-2497-2016>.
- 382 Inai, Y., M. Shiotani, M. Fujiwara, F. Hasebe, and H. Vömel (2015), Altitude misestimation
383 caused by the Vaisala RS80 pressure bias and its impact on meteorological profiles, *Atmos.*
384 *Meas. Tech.*, 8, 4043–4054, <https://doi.org/10.5194/amt-8-4043-2015>.
- 385 Livesey, N. J., et al. (2018), Version 4.2x-3.1 Level 2 data quality and description document, JPL
386 D-33509 Rev. B. [Available at [https://mls.jpl.nasa.gov/data/v4-](https://mls.jpl.nasa.gov/data/v4-2_data_quality_document.pdf)
387 [2_data_quality_document.pdf](https://mls.jpl.nasa.gov/data/v4-2_data_quality_document.pdf).]
- 388 McPeters, R., Kroon, M., Labow, G., Brinksma, E., Balis, D., Petropavlovskikh, I., Veefkind, J.
389 P., Bhartia, P. K., and Levelt, P. F. (2008), Validation of the Aura Ozone Monitoring

390 Instrument total column ozone product, *J. Geophys. Res.*, 113, D15S14,
391 doi:10.1029/2007JD008802.

392 McPeters, R. D., and G. J. Labow (2012), Climatology 2011: An MLS and sonde derived ozone
393 climatology for satellite retrieval algorithms, *J. Geophys. Res.*, 117, D10303,
394 doi:10.1029/2011JD017006. McPeters, R. D., Frith, S., and Labow, G. J. (2015), OMI total
395 column ozone: extending the long-term data record, *Atmos. Meas. Tech.*, 8, 4845–4850,
396 <https://doi.org/10.5194/amt-8-4845-2015>.

397 McPeters, R., Frith, S., Kramarova, N., Ziemke, J., and Labow, G. (2019), Trend quality ozone
398 from NPP OMPS: the version 2 processing, *Atmos. Meas. Tech.*, 12, 977–985,
399 <https://doi.org/10.5194/amt-12-977-2019>.

400 Morris, G. A., W. D. Komhyr, J. Hirokawa, J. Flynn, B. Lefer, N. Krotkov, F. Ngan (2010), A
401 balloon sounding technique for measuring SO₂ plumes, *J. Atmos. Oceanic Technol.*, 27,
402 1318–1330. doi: 10.1175/2010JTECHA1436.1

403 Smit, H. G. J., et al. (2007), Assessment of the performance of ECC-ozonesondes under quasi-
404 flight conditions in the environmental simulation chamber: Insights from the Jülich Ozone
405 Sonde Intercomparison Experiment (JOSIE), *J. Geophys. Res.*, 112, D19306,
406 doi:10.1029/2006JD007308.

407 Smit, H. G. J., and the Panel for the Assessment of Standard Operating Procedures for
408 Ozonesondes (ASOPOS) (2012), Guidelines for homogenization of ozonesonde data,
409 SI2N/O3S-DQA activity as part of “Past changes in the vertical distribution of ozone
410 assessment”. [Available at [http://www-](http://www-das.uwyo.edu/%7Edeshler/NDACC_O3Sondes/O3s_DQA/O3S-DQA-Guidelines%20Homogenization-V2-19November2012.pdf)
411 [das.uwyo.edu/%7Edeshler/NDACC_O3Sondes/O3s_DQA/O3S-DQA-](http://www-das.uwyo.edu/%7Edeshler/NDACC_O3Sondes/O3s_DQA/O3S-DQA-Guidelines%20Homogenization-V2-19November2012.pdf)
412 [Guidelines%20Homogenization-V2-19November2012.pdf](http://www-das.uwyo.edu/%7Edeshler/NDACC_O3Sondes/O3s_DQA/O3S-DQA-Guidelines%20Homogenization-V2-19November2012.pdf).]

- 413 Smit, H. G. J., and the Panel for the Assessment of Standard Operating Procedures for
414 Ozonesondes (ASOPOS) (2014), Quality assurance and quality control for ozonesonde
415 measurements in GAW, World Meteorological Organization, GAW Report 201. [Available
416 at http://www.wmo.int/pages/prog/arep/gaw/documents/FINAL_GAW_201_Oct_2014.pdf.]
- 417 Stauffer, R. M., G. A. Morris, A. M. Thompson, E. Joseph, G. J. R. Coetzee, and N. R. Nalli
418 (2014), Propagation of radiosonde pressure sensor errors to ozonesonde measurements,
419 *Atmos. Meas. Tech.*, 7, 65–79, doi:10.5194/amt-7-65-2014.
- 420 Steinbrecht, W., H. Claude, F. Schönenborn, U. Leiterer, H. Dier, H., and E. Lanzinger (2008),
421 Pressure and temperature differences between Vaisala RS80 and RS92 radiosonde systems,
422 *J. Atmos. Ocean. Tech.*, 25, 909-927, doi:10.1175/2007JTECHA999.1.
- 423 Sterling, C. W., Johnson, B. J., Oltmans, S. J., Smit, H. G. J., Jordan, A. F., Cullis, P. D., et al.
424 (2017). Homogenizing and estimating the uncertainty in NOAA’s long term vertical ozone
425 profile records measured with the electrochemical concentration cell ozonesonde. *Atmos.*
426 *Meas. Tech.*, 11, 3661-3687, <https://doi.org/10.5194/amt-2017-397>
- 427 Tarasick, D. W., J. Davies, H. G. J. Smit, and S. J. Oltmans (2016), A re-evaluated Canadian
428 ozonesonde record: Measurements of the vertical distribution of ozone over Canada from
429 1966 to 2013, *Atmos. Meas. Tech.*, 9, 195–214, doi:10.5194/amt-9-195-2016.
- 430 Thompson, A. M., J. C. Witte, H. G. J. Smit, S. J. Oltmans, B. J. Johnson, V. W. J. H. Kirchhoff,
431 and F. J. Schmidlin (2007), Southern Hemisphere Additional Ozonesondes (SHADOZ)
432 1998–2004 tropical ozone climatology: 3. Instrumentation, station-to-station variability, and
433 evaluation with simulated flight profiles, *J. Geophys. Res.*, 112, D03304,
434 doi:10.1029/2005JD007042.

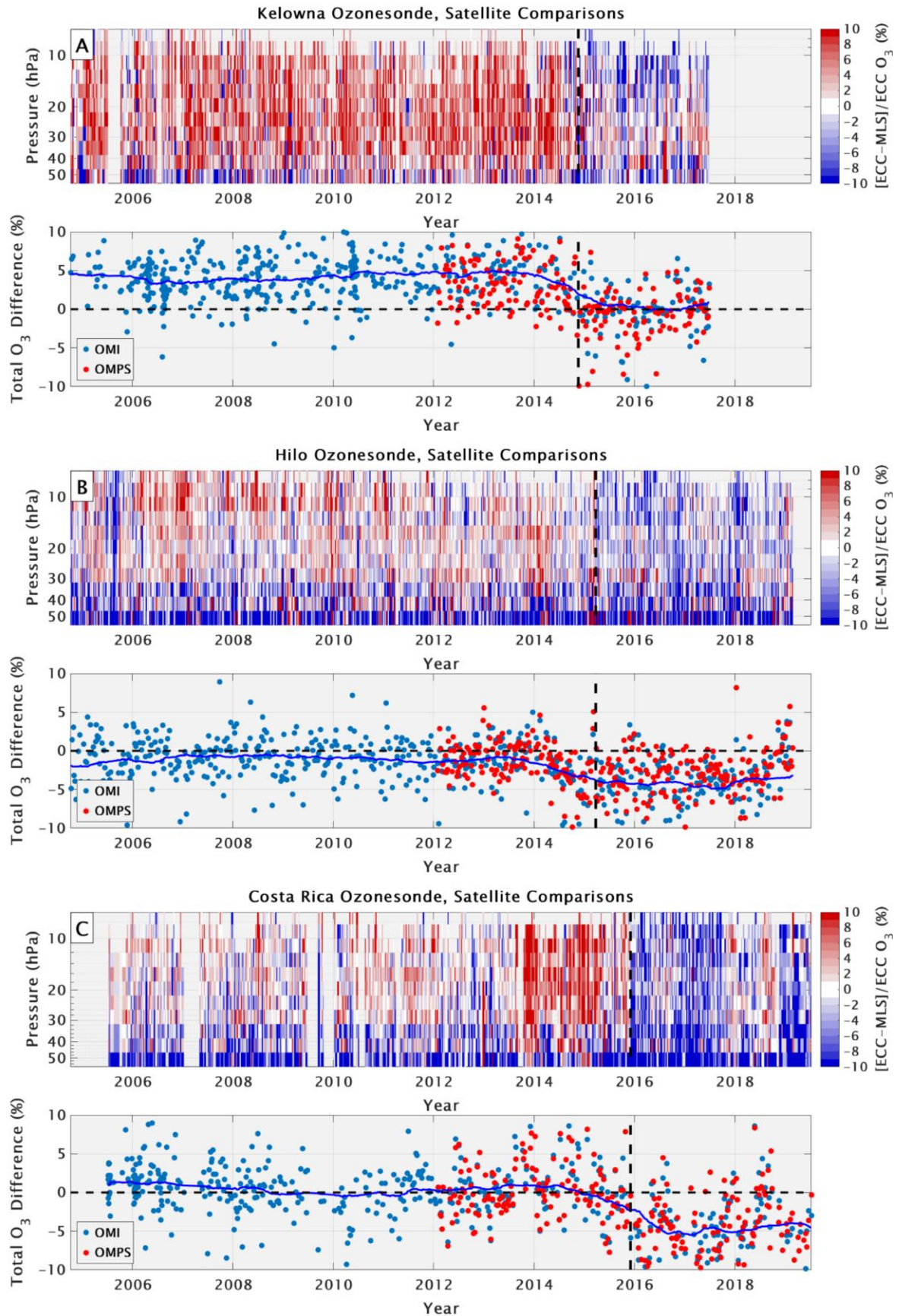
- 435 Thompson, A. M., Witte, J. C., Sterling, C., Jordan, A., Johnson, B. J., Oltmans, S. J., et al.
436 (2017). First reprocessing of Southern Hemisphere Additional Ozonesondes (SHADOZ)
437 profiles (1998-2016). 2. Comparisons with satellites and ground-based instruments, *J.*
438 *Geophys. Res. Atmos.*, 122, 13000-13025, <https://doi.org/10.1002/2017JD27406>
- 439 Thompson, A. M., H. G. J. Smit, J. C. Witte, R. M. Stauffer, B. J. Johnson, G. Morris, et al.
440 (2019), Ozonesonde quality assurance: The JOSIE-SHADOZ (2017) Experience, *Bull. Amer.*
441 *Met. Soc.*, 100 (1), 155-171, <https://doi.org/10.1175/BAMS-D-17-0311.1>
- 442 Van Malderen, R., Allaart, M. A. F., De Backer, H., Smit, H. G. J., and De Muer, D. (2016). On
443 instrumental errors and related correction strategies of ozonesondes: Possible effect on
444 calculated ozone trends for the nearby sites Uccle and De Bilt. *Atmos. Meas. Tech.*, 9, 3793–
445 3816. <https://doi.org/10.5194/amt-9-3793-2016>.
- 446 Witte, J. C., Thompson, A. M., Smit, H. G. J., Fujiwara, M., Posny, F., Coetzee, G. J. R., et al.
447 (2017). First reprocessing of Southern Hemisphere ADditional Ozone-sondes (SHADOZ)
448 profile records (1998–2015): 1. Methodology and evaluation. *J. Geophys. Res. Atmos*, 122,
449 6611–6636. <https://doi.org/10.1002/2016JD026403>.
- 450 Witte, J. C., Thompson, A. M., Schmidlin, F. J., Northam, E. T., Wolff, K. R., and Brothers, G.
451 B. (2019). The NASA Wallops Flight Facility digital ozonesonde record: Reprocessing,
452 uncertainties, and dual launches. *Journal of Geophysical Research: Atmospheres*, 124, 3565–
453 3582. <https://doi.org/10.1029/2018JD030098>
- 454 WMO/GAW Ozone Monitoring Community: World Meteorological Organization-Global
455 Atmosphere Watch Program (WMO-GAW)/World Ozone and Ultraviolet Radiation Data
456 Centre (WOUDC) [Data] (2015), available at: <https://woudc.org> (last access: 25 September
457 2019), <https://doi.org/10.14287/10000008>
- 458

459 Table 1. ECC type, total number of samples, latitude, longitude, Solution type (SST) (KI
 460 concentration, buffer strength), the 25th percentile, mean, and 75th percentile TCO differences
 461 with OMI (October 2004-present), date of drop-off and maximum amount of drop-off in the 100-
 462 sample moving mean (see Figure 1) if applicable, and ground-based instrument if applicable are
 463 listed. Sites with a > 3 % drop in TCO relative to OMI (Section 2.3) are in bold. Type1 is EnSci
 464 (Westminster, CO, USA) and Type2 is Science Pump Corporation (SPC; Camden, NJ, USA).
 465 Note that Japanese stations Sapporo, Tateno, and Naha launched carbon-iodine ozonesondes
 466 prior to 2008-2009, and those are not considered here.

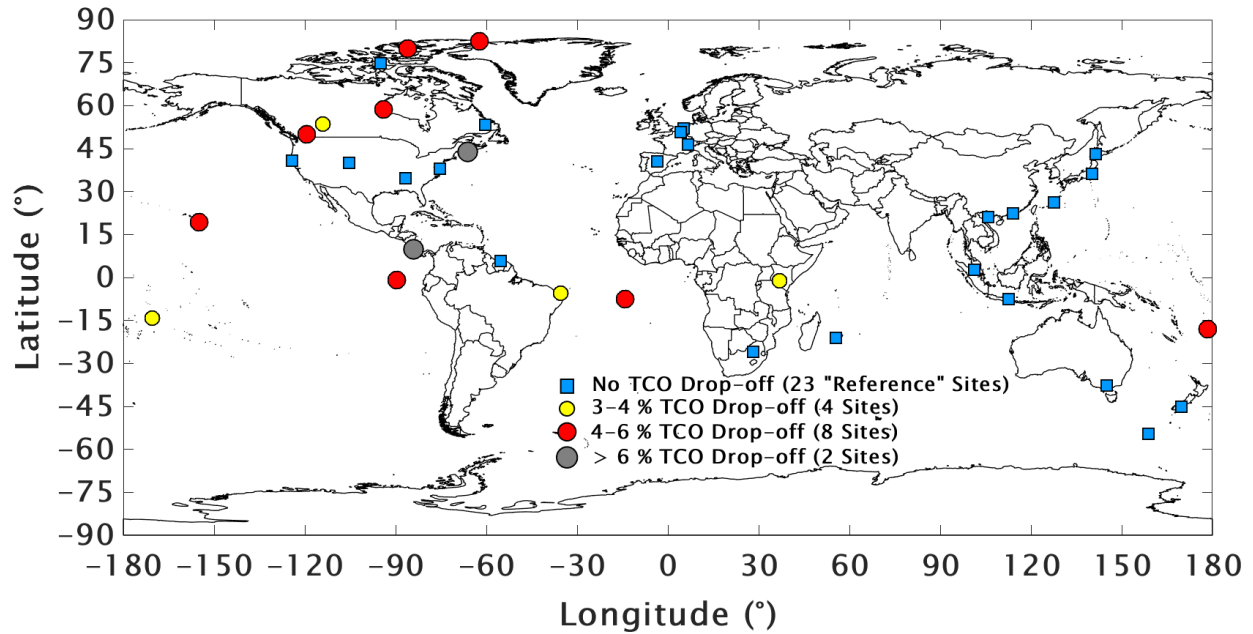
Site	ECC	N	Lat (°)	Lon (°)	KI SST	OMI 25th (%)	OMI μ (%)	OMI 75th (%)	Drop-Off	TCO Drop (%)	Ground TCO
Alert	Type1	645	82.49	-62.34	1.0%, Full	-0.6	1.0	3.1	02/2016	-4.3	Brewer
Eureka	Type1	922	79.98	-85.94	1.0%, Full	-0.4	1.9	4.5	04/2016	-4.2	Brewer
Resolute	Type1	540	74.7	-94.96	1.0%, Full	-4.8	-2.2	0.6	N/A	N/A	Brewer
Churchill	Type1	417	58.74	-94.07	1.0%, Full	-1.1	0.7	3.3	11/2016	-5.5	Brewer
Edmonton	Type1	674	53.54	-114.1	1.0%, Full	-2.9	-0.4	2.9	01/2017	-3.9	Brewer
Goose Bay	Type1	663	53.31	-60.36	1.0%, Full	-1.9	0.7	3.4	N/A	N/A	Brewer
De Bilt	Type2	736	52.1	5.18	1.0%, Full	-0.6	1.3	2.9	N/A	N/A	Brewer
Uccle	Type1	2140	50.8	4.35	0.5%, Half	-1.5	0.0	2.0	N/A*	N/A	Brewer
Kelowna	Type1	664	49.93	-119.4	1.0%, Full	1.4	3.4	5.9	11/2014	-4.7	N/A
Payerne	Type1	2191	46.49	6.57	0.5%, Half	-2.5	-0.7	0.9	N/A*	N/A	N/A
Yarmouth	Type1	616	43.87	-66.11	1.0%, Full	-0.2	2.4	5.3	02/2015	-7.4	N/A
Sapporo	Type1	373	43.06	141.33	0.5%, Half	1.0	2.7	4.4	N/A	N/A	Dobson
Trinidad Head	Type1	772	40.8	-124.16	1.0%, 1/10	-2.1	-0.2	1.6	N/A	N/A	N/A
Madrid	Type2	680	40.47	-3.58	1.0%, Full	-2.1	-0.3	1.6	N/A	N/A	Brewer
Boulder	Type1	816	40	-105.25	1.0%, 1/10	-2.1	-0.3	2.0	N/A	N/A	Dobson
Wallops Island	Type2	773	37.93	-75.48	1.0%, Full	-2.5	-0.3	1.8	N/A	N/A	Dobson
Tateno	Type1	430	36.06	140.13	0.5%, Half	0.8	2.6	4.3	N/A	N/A	Dobson, Brewer
Huntsville	Type1	759	34.72	-86.64	1.0%, 1/10	-1.6	0.0	1.9	N/A	N/A	N/A
Naha	Type1	403	26.21	127.69	0.5%, Half	0.2	1.7	3.5	N/A	N/A	Dobson
Hong Kong	Type2	690	22.31	114.17	1.0%, Full	-7.0	-4.6	-2.1	N/A	N/A	N/A
Hanoi	Type1	264	21.01	105.8	0.5%, Half	-4.1	-1.8	0.5	N/A	N/A	N/A
Hilo	Type1	711	19.43	-155.04	1.0%, 1/10	-3.7	-1.9	0.2	03/2015	-4.0	Dobson, Brewer
Costa Rica	Type1	605	9.94	-84.04	1.0%, 1/10	-3.1	-0.8	1.9	12/2015	-6.2	N/A
Paramaribo	Type2	517	5.8	-55.21	1.0%, Full	-5.0	-2.5	-0.1	N/A	N/A	Brewer
Kuala Lumpur	Type1	264	2.73	101.27	0.5%, Half	-7.3	-4.5	-1.3	N/A	N/A	N/A
San Cristobal	Type1	168	-0.92	-89.62	1.0%, 1/10	-4.9	-0.8	2.4	01/2014	-4.7	N/A
Nairobi	Type1	596	-1.27	36.8	0.5%, Half	-3.7	-2.1	-0.4	07/2016	-3.2	N/A
Natal	Type2	400	-5.42	-35.38	1.0%, Full	-3.6	-1.5	1.0	04/2016	-3.5	Dobson
Watukosek	Type1	115	-7.5	112.6	2.0%, None	-3.4	-1.9	0.4	end 10/2013	N/A	N/A
Ascension	Type1	394	-7.58	-14.24	0.5%, Half	-6.0	-2.8	0.4	03/2016	-4.2	N/A
Samoa	Type1	474	-14.23	-170.56	1.0%, 1/10	-3.0	-1.2	0.9	07/2016	-3.9	Dobson
Fiji	Type1	200	-18.13	178.4	1.0%, 1/10	-3.1	-0.5	2.2	05/2015	-4.8	N/A
Réunion	Type1	449	-21.06	55.48	0.5%, Half	-2.0	0.3	2.4	N/A	N/A	SAOZ
Irene	Type2	212	-25.9	28.22	1.0%, Full	-1.3	1.3	4.3	N/A	N/A	Dobson

Broadmeadows	Type2	667	-37.69	144.95	1.0%, Full	-0.9	0.6	2.7	N/A	N/A	Dobson
Lauder	Type1	705	-45	169.68	0.5%, Half	-3.3	-1.3	0.8	N/A	N/A	Dobson
Macquarie	Type2	675	-54.5	158.95	1.0%, Full	-4.6	-2.4	0.1	N/A	N/A	Dobson

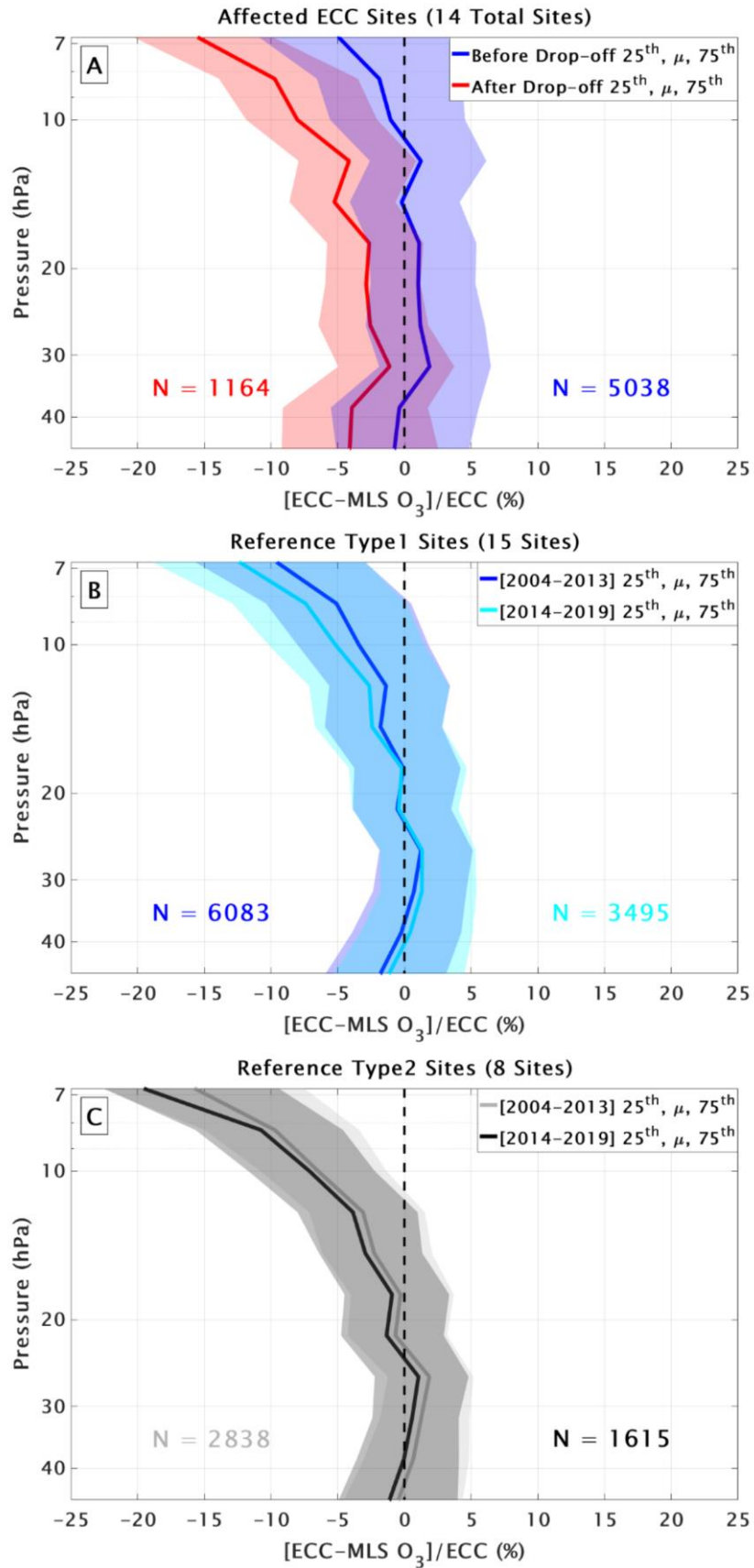
467



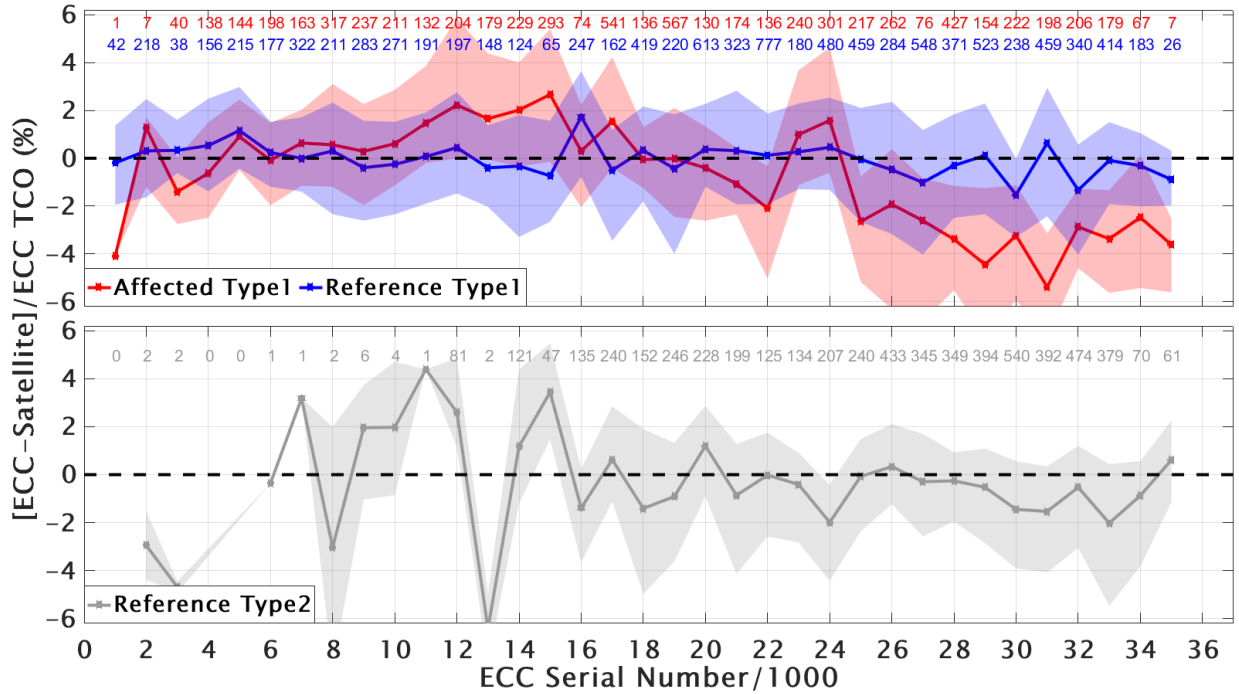
469 Figure 1. Time series of comparisons at Kelowna (A; data end in June 2017), Hilo (B), and Costa
470 Rica (C) between ECC ozonesondes and Aura MLS stratospheric O₃ profiles (top panels), and
471 OMI (blue dots) and OMPS (red dots) TCO (bottom panels). Red or blue colors on the top panels
472 indicate where the ECC O₃ is greater or less than MLS. Horizontal dashed lines indicate the 0 %
473 line for TCO comparisons. Vertical dashed lines indicate the date of the drop-off at each site (see
474 Table 1 for dates), marked by a TCO drop of 3 % relative to the 2004-2013 average difference in
475 OMI and ECC TCO comparisons (blue line on bottom panels).
476



477
 478 Figure 2. Map of all 37 ECC ozonesonde sites considered in this study. The blue squares indicate
 479 sites that show no detectable TCO drop-off relative to OMI. We call these sites “reference” sites.
 480 The yellow, red, and grey dots indicate sites that exhibit maximum drops of 3-4 %, 4-6 %, and
 481 over 6 % (Table 1) relative to OMI TCO. The method for computing the values shown on this
 482 figure and in Table 1 are explained in Section 2.3.
 483



485 Figure 3. A composite of comparisons between ECC ozonesonde and Aura MLS stratospheric O₃
486 profiles from before the drop-off at each site (A; blue; dates of drop-off are in Table 1), and
487 during the period after the drop-off (red). Reference Type1 (B) and Type2 (C) sites were split
488 into 2004-2013 and 2014-2019 comparisons to show that there has been no comparable drop-off
489 in stratospheric O₃ around the same period. The shading indicates the 25th to 75th percentile, with
490 mean values shown by the solid lines. ECC sonde sample numbers are shown for each period in
491 the lower portion of the figure.
492



493
 494 Figure 4. Median (lines) and 25th to 75th (shading) percentiles of comparisons between ECC and
 495 OMI and OMPS TCO. The comparisons are separated by every 1000 serial numbers for Type1
 496 (top) and Type2 (bottom) ECCs. The Type1 ECCs are separated into affected (red) and reference
 497 (blue) stations. Natal, the only affected Type2 site, is not included in this figure. The number of
 498 samples for each serial number bin are shown at the top of each panel.
 499
 500